The use of X-ray line profile analysis in the tetragonal to monoclinic phase transformation of ball milled, as-sintered and thermally aged zirconia powders

JYUNG-DONG LIN, JENQ-GONG DUH
Department of Materials Science and Engineering, National Tsing Hua University, Hsinchu, Taiwan

The martensitic tetragonal to monoclinic (t → m) transformation in zirconia plays an important role in determining the mechanical properties and low temperature degradation of this ceramic. The analysis of X-ray data using the Warren–Averbach procedure can supply reliable information about crystallite size and microstrain under various conditions. The X-ray line profile analysis results can shed light on the martensitic transformation and the microstructural evolution of the t and m phases. The presence of m plates causing the formation of partially transformed t crystals reduces the mean size of the t crystals. The ball milling process also affects the mean size of the produced monoclinic crystals. The microstrain of the t and m phases can also be influenced by the ball milling and also by matrix constraints. Zirconia powders doped with low contents of CeO_2 exhibit an isothermal type t → m transformation during thermal annealing which affects the subsequent athermal transformation upon cooling and thus a decrease in the mean size of the m crystals is produced.

1. Introduction

The mechanical behaviour of zirconia based ceramics is an area that has received a considerable amount of attention in recent years [1, 2]. Unfortunately, the tendency for low temperature degradation in zirconia limits the use of these materials [3]. The reason why zirconia has excellent mechanical properties whilst at the same time being susceptible to water containing environments at low temperatures is associated with its tetragonal to monoclinic (t → m) phase transformation. This martensitic t → m phase transformation can be initiated by thermal or mechanical processes. In the case of ZTA (zirconia toughened alumina) powders, a "size" effect has been isolated and its significance on the t → m transition has been discussed [4–7].

One characteristic of the martensitic phase transformation is that the produced monoclinic phase crystals are closely related to the parent tetragonal phase crystals. The analysis of X-ray powder diffraction data using the Warren–Averbach line profile broadening technique can non-destructively probe the microstructure of materials [8, 9]. The application of this technique to probe the microstructural relationship between the t and m phases will provide data that will supplement data collected by several other techniques. Usually the area-weighted mean crystallite size $\langle D \rangle_a$ is sensitive to the existence of fine crystals, and thus it can be used to probe the presence of partially transformed t crystals. It is reported in the literature that the m phase usually forms in a plate or lath shape and thus partitions the t crystals which results in a decrease in the mean t crystallite size [10–14]. Consequently, if the t → m phase transformation occurs in a dense TZP (Tetragonal Zirconia Polycrystal) matrix, an autocatalytic phase transformation would take place, in which the preferred t crystals tend to be transformed into the m phase [11, 15]. Therefore, according to the martensitic characteristics and the results of X-ray line profile analysis, the microstructural evolution of the t and m phases in the t → m phase transformation can be revealed.

This study investigates the t → m phase transformation of ultrafine zirconia powders in three different states including ball milled and thermally aged samples using the Warren–Averbach (W–A) profile analysis technique and other simplified methods [9, 16, 17]. This work is part of a continuing programme performed in our laboratory on the development of Y_2O_3–CeO_2–ZrO_2 ceramics [18–23]. A recent study focused on the analysis of X-ray diffraction data in order to investigate the size distribution and microstrain of as-fabricated powders [9]. In this paper, the occurrence of the t → m phase transformation including the as-sintered surface of a dense body is discussed. These data provide a better understanding of the transition mechanism of the t → m phase transformation for ultrafine t crystallites in a non-constrained particle and also a compacted green body.

0022–2461

2. Experimental procedure

Various coprecipitation methods including ammonia-coprecipitation and urea hydrolysis were used to produce ultrafine zirconia powders. $ZrOCl_2 \cdot 8H_2O$, $Ce(NO_3)_3 \cdot 6H_2O$, and $Y(NO_3)_3 \cdot 5H_2O$ (Merck, Darmstadt, Germany) were used in a stock solution that had a cation concentration of 0.5 M. Then concentrated ammonia solution ($\sim$25%) and the stock solution were dropped into a well-stirred NH_4OH solution, and the pH was maintained above 10.8 at all times to ensure complete reaction. The urea hydrolysis process consisted of boiling the stock solution (0.1 M) with 0.42 M urea for 5 h which produced a white colloidal solution. These gels were filtered by a tube pump washed with alcohol and washed a further two times with deionized water. A subsequent calcination and hydrothermal treatment (HTX) were performed to produce crystallization. The full powder preparation details are reported elsewhere [8].

An analysis of the X-ray powder diffraction data using the Warren–Averbach procedure was performed to evaluate the mean crystallite size, crystallite size distribution and microstrain in the zirconia powders. The X-ray powder diffractometer produced Ni-filtered CuK_α radiation from a 18 KW self-rotated anode X-ray generator (MXP18, MAC Science, Tokyo, Japan) operated at 40 KV and 20 mA. The data were collected in 0.02° steps between 26–32° and 55–65° with counting times of 3 and 6 s respectively. The X-ray profiles were analysed using a software program developed by MAC. Science, Corp. (Tokyo, Japan). The volume fraction of the monoclinic phase, V_m, was evaluated using the method of Toraya *et al.* [24].

$$V_m = \frac{1.311X_m}{1 + 0.311X_m} \quad (1)$$

$$X_m = \frac{I_{(\bar{1}11)_m} + I_{(111)_m}}{I_{(111)_t} + I_{(\bar{1}11)_m} + I_{(111)_m}} \quad (2)$$

where X_m is the integrated intensity ratio, and the subscripts m and t represent the intensities of the m and t phases after the peak separation and fitting procedures. A detailed discussion of the X-ray fitting procedures is presented elsewhere [9].

The crystallite sizes and microstrains of the t and m phases in ultrafine zirconia powders in ball milled samples, sintered bulk samples and thermally aged samples were investigated. The ball milled powders were prepared by ball milling ammonia-derived powders with the compositions 5.5 mol % CeO_2 and 2 mol % $YO_{1.5}$, that had been calcined at 500 °C for 0.5 h, in alcohol for 12 h. Subsequently the ball milled powders were uniaxially cold-pressed into pellets of 1 cm diameter under a pressure of $\sim$160 MPa and then sintered at 1500 °C for 2 h in air. These dense zirconia bulk samples were used to probe the occurrence of the t $\rightarrow$ m phase transformation in the as-sintered surface. The powders doped with 3, 5.5 and 7 mol % CeO_2 were used in thermal ageing tests in the form of pellets that were produced by cold pressing at $\sim$50 MPa which is a sufficiently low pressure to avoid introducing strains into the pellets.

3. Results and discussion

3.1. Milled powders

Since the t $\rightarrow$ m phase transformation in zirconia is stress-induced, the metastable tetragonal phase can be transformed into the monoclinic phase by the ball milling [25, 26]. Murase and Kato have reported that the presence of water vapour can enhance the occurrence of the t $\rightarrow$ m phase transformation [26]. In order to eliminate this water vapour effect, the powders were ball-milled for 12 h in absolute alcohol to produce the powder properties listed in Table I. The amount of m phase in powders A1, A2, and A3 after a 12 h ball milling increased by 8.3, 9.5 and 13.8 vol % respectively. The mean crystallite sizes, $\langle D \rangle_a$, of the t phase slightly decreased, while that of the m phase increased. In general, the rate of size reduction in dense hard particles rapidly decreases if the mean size is less than 1 μm [27]. Thus, the ball milling operation does not reduce the size of the small crystals but nearly produces deagglomerate ion to produce ultrafine powders. This point is supported by the Brunauer–Emmett–Teller (BET) surface area measurement, that shows an increase in the powder surface area from 96.7 to 110.3 $m^2 g^{-1}$ after the 12 h ball milling.

There is no appreciable change in the t phase microstrain whereas that of the m phase doubles after the 12 h ball milling. Van Riessen and O'Connor [28] have reported that the m phase microstrain is larger than that of the t phase for an Al_2O_3–ZrO_2 composite, in which the dispersed ZrO_2 particles are constrained in the Al_2O_3 matrix. In this case the extent of t phase transformation is restricted and thus an increase in the microstrain of the m phase is created. However, a transformed t crystal can expand freely in the case of isolated particles and thereby relieve the majority of the microstrain in the m phase. Consequently in the case of isolated particles the observed microstrain for the m phase is slightly smaller than that of the parent t phase .

Heuer and Rühle [29] and Rühle and Heuer [30] have demonstrated that the kinetics of the martensitic t $\rightarrow$ m transformation in ZrO_2 are nucleation-controlled and that nucleation is always stress-assisted, even when the transformation occurs spontaneously. Therefore, the autocatalytic transformation occurs in a dense matrix and the derived product phase tends to exhibit a preferred orientation. For an isolated particle without any matrix constraint, the growth of the product crystal is limited to be inside the crystal of the parent phase which results in a smaller size for the produced m phase than the parent t phase. However, partial transformation is often observed in Ce–TZP and Y–TZP grains, and this may produce a similar stress in the nucleation and propagation states of the m phase [11]. In this study, the m phase has two forms: one thermally-induced and the other stress-induced. The former is formed during crystallization, whereas the latter is due to the effect of milling. The nature of the thermally-induced m phase depends mainly on the crystallization process and its crystallite size is, as previously reported [9], slightly smaller than that of the t phase. This is consistent with the results of Srinivasan *et al.* [31], in which the ratio of D_t/D_m

TABLE I The volume percentage of tetragonal phase, mean crystallite size, and microstrain of 5.5 mol % CeO_2 – 2 mol % $YO_{1.5}$ – ZrO_2 powders before and after a 12 h ball milling

Sample designation	Tetragonal content (vol %)	Tetragonal phase $2w_{Pv(L)}$[a] (nm)	Tetragonal phase Crystallite size $\langle D\rangle_a$[b] (nm)	Tetragonal phase Microstrain $\langle\varepsilon^2\rangle^{1/2}_{L=3.0\,nm}$[b] ($\times 10^2$)	Monoclinic phase $2w_{Pv(L)}$ (nm)	Monoclinic phase Crystallite size $\langle D\rangle_a$ (nm)	Monoclinic phase Microstrain $\langle\varepsilon^2\rangle^{1/2}_{L=3.0\,nm}$ ($\times 10^2$)
A1	68.2	6.92	5.92	1.97	5.46	4.86	0.46
$A1_{milled}$	59.9	6.70	5.12	2.00	4.99	5.10	2.63
A2	70.3	7.18	5.39	2.10	3.99	4.58	1.26
$A2_{milled}$	60.8	7.90	5.18	2.19	4.79	4.73	2.68
A3	69.6	6.99	5.48	2.11	3.95	4.54	–
$A3_{milled}$	55.8	7.66	5.29	2.05	6.99	5.26	2.81

[a] The full-width of volume-weighted crystallite size distribution at half maximum.
[b] The area-weighted mean crystallite size and microstrain are calculated using the Warren–Averbach procedure.

decreases with an increase in the calcination time at 500 °C. In this study the t phase is initially formed which is transformed into the m phase at the longer time periods. If the powders are polydomained, a primary particle with a diameter of ~10.0 nm will, according to BET data [9], contain 8 crystals with a diameter of ~5.0 nm. The evaluated microstrain of the m phase is smaller than that of the t crystal. We believe that the majority of the crystals in the thermally-induced m phase exist in a rather isolated state.

As the t → m transition occurs, the volume of the lattice of the parent phase must expand by 5 vol % and the plates or laths of the m phase must grow and partition the parent t matrix. In other words, the crystallite size of the derived m phase will be constrained by the matrix boundaries and other m plates or laths. This leads to a broadening in the size distribution of the m crystals.

The influence of the stress produced by the ball milling is different on the two phases. The accumulated t phase stress can be eliminated by the t → m phase transformation, whereas that of m phase remains stored in the crystal lattice. Therefore, the microstrain, $\langle\varepsilon^2\rangle^{1/2}_{L=3.0\,nm}$, of the m phase increases from 1.0×10^{-2} into 2.68×10^{-2} and is larger than that observed for the t phase after the 12 h ball milling. Morosin *et al.* [32] have shown that the m phase microstrain increased as the shock pressure increased upto a maximum value. In these experiments the samples were subjected to a controlled shock compression using "Bear" explosive-loading fixtures. It should be noted that Morosin *et al.* did not observe any anisotropy in the properties of the m phase after the shock. This is in agreement with data currently reported in the literature [9].

When nucleation on the surface of the t crystals is produced by the stress imposed by the ball milling, then the plates or laths of the m phase quickly grow inwards into the parent phase and partition t crystals, thereby producing a decrease in the mean crystallite size of the t phase. Alternatively, pre-existing and/or the newly formed m plates can grow into larger plates and thus the mean size of the m phase is increased. As is shown in Table I, the crystallite size of the t phase decreases, whilst the size increase in the m phase becomes more pronounced as the amount of transformed t phase increases. On the other hand, the distribution of the m crystallite size is broadened as is shown in Table I, whilst that of the t crystallite size is only slightly altered. Fig. 1 (a and b) represent the distributions of the volume-weighted crystallite size, $P_v(L)$, of the t and m phases in sample A3 both before and after the ball milling. The distribution of the t phase moves towards low L values and the width is slightly changed, whereas that of the m phase shifts to higher L values and the width becomes broader. It can be seen from Fig. 1b that the volume percentage of the m phase is originally 30% which increases by nearly 10%. Thus, the total fractional change is 25%, and thus ball milling significantly changes the m phase

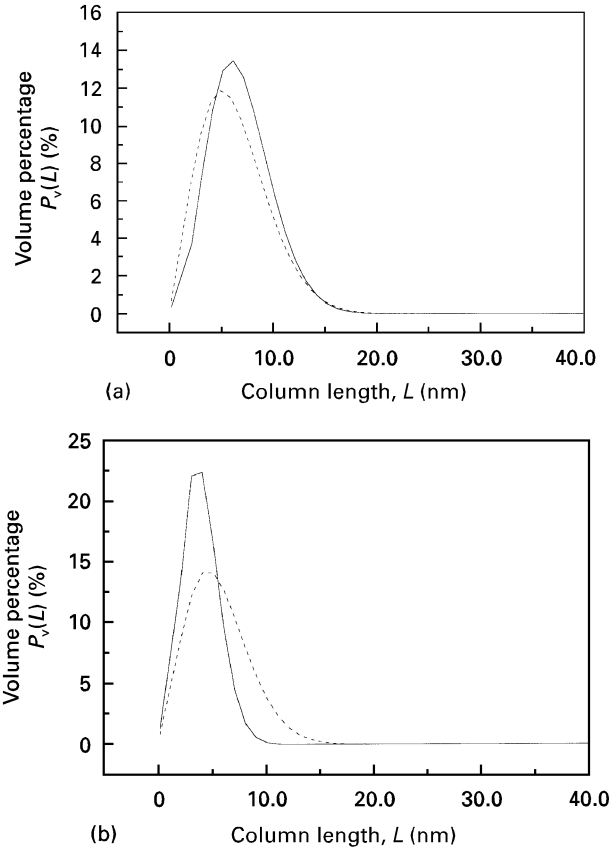

Figure 1 The distribution of the volume weighted crystallite size $P_v(L)$ of the (a) tetragonal and (b) monoclinic phases as a function of column length, (L), for samples (—) A3 and (---) $A3_{milled}$.

content. If the mechanism for stress-induced phase transformation due to ball milling is similar to that for the thermally-induced transformation, then, the mean value and the distribution of the crystallite size for the m phase would not change as the transformation progressed. Thus the mechanism for stress-induced transformation may be postulated to be that the transformation proceeds by the growth of either pre-existing m plates or newly nucleated plates, and both can grow into larger plates due to the randomly applied stress of ball milling. Therefore, the mean size of the m phase increases after 12 h of ball milling.

3.2. As-sintered surface of 5.5 mol % CeO_2–2 mol % $YO_{1.5}$–ZrO_2

The surfaces of as sintered samples were analysed by X-ray diffraction (XRD), as shown in Fig. 2a. If the sintering temperature is raised from 900 to 1300 °C, then the t phase in the free surface partially transforms into the m phase, which tends to form in a preferred $(\bar{1}11)_m$ orientation. This results in an increase in the ratio $I_{(\bar{1}11)m}/I_{(111)m}$ from 2.47 to 5.62 as the sintering temperature is raised from 1300 to 1500 °C. Preferred orientations or textured surfaces have been previously reported for as-sintered, fractured, and ground zirconia based samples [14, 33].

Fig. 2(b and c) show the crystallite size and microstrain as a function of the sintering temperature calculated by the Warren–Averbach method ($\langle D\rangle_a$ and $\langle\varepsilon^2\rangle^{1/2}$) and single peak methods (D_β and $\hat{e}$ or D_c and G) volume-weighted mean crystallite size Δ_β and microstrain $\hat{e}$ derived by de Keijser's method or mean crystallite size D_c and strain constant G derived by Cohen's method [9]. All the methods agree that the mean crystallite size of the t phase decreases in the presence of the m phase at 1300 °C and then increases as the sintering temperature is raised to 1400 °C. The crystallite size of the m phase increases as the sintering temperature increases. Since partially transformed t crystals are often observed in Y–TZP and Ce–TZP [10–14], it is argued that the t-matrix is partitioned due to the growth of m plates or laths which results in a decrease in the space for further m phase formation [14] and the growth of new m plates is impeded by pre-existing m plates or laths. This leads to a decrease in the mean crystallite size of the t phase and the crystallite size of the m phase is usually less than that of the t phase. It should be noted that the t phase crystals continue to grow as the sintering temperature is raised from 1300 and 1500 °C. If the t → m phase transformation occurs on the surface of sintered samples during cooling, i.e., the t crystals grow first and are subsequently transformed, the crystallite size of t phase in the samples sintered at 1400 and 1500 °C would decrease similar to the case for the 1300 °C sample since the new m plates grow and partition the growing t crystals. This, however, contradicts the observed behaviour for the crystallite size, i.e., the size of the t crystals increases as the sintering temperature is raised from 1300 to 1500 °C, as indicated in Fig. 2b. Therefore, the m phase must form during the heating stage and in this study, it happens at temperatures

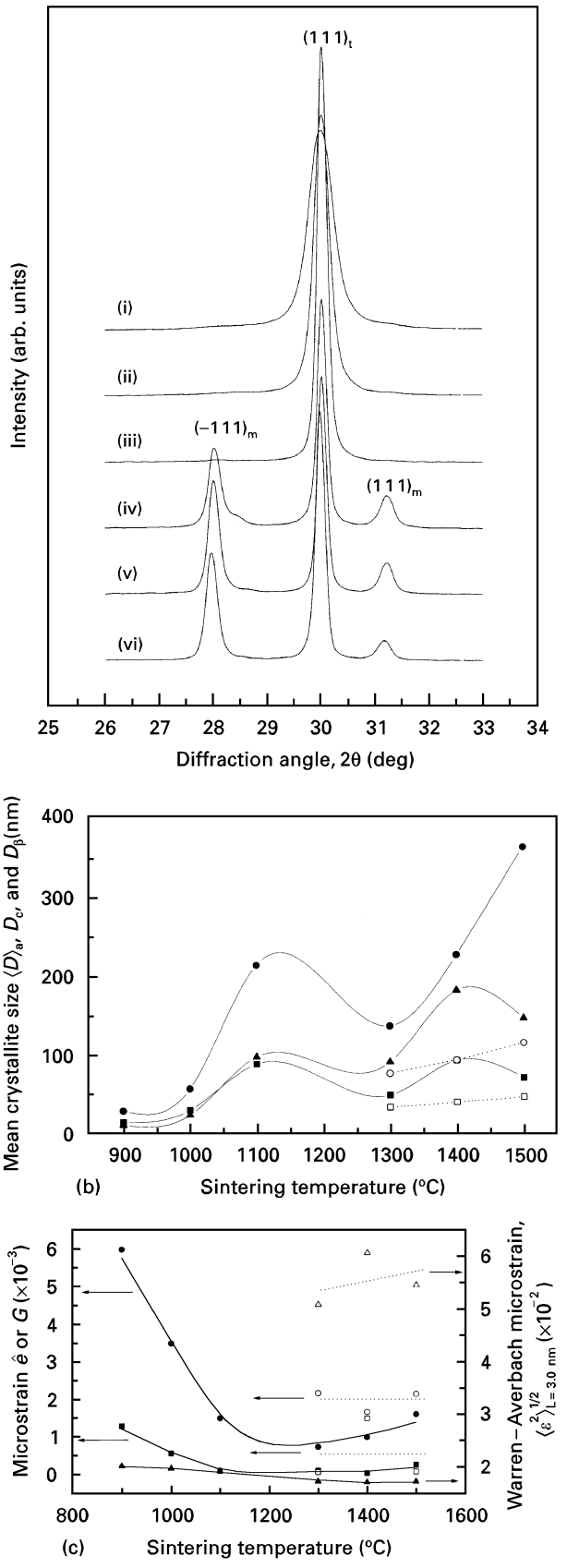

Figure 2 (a) XRD profiles of the as-sintered surface for 5.5 mol % CeO_2–2 mol % $YO_{1.5}$–ZrO_2 samples sintered at (i) 900 °C, (ii) 1000 °C, (iii) 1100 °C, (iv) 1300 °C, (v) 1400 °C and (vi) 1500 °C for 2 h. and (b) Mean crystallite size of sample A-X12 as a function of sintering temperature. Solid symbols and solid line correspond to the t phase, whereas open symbol and dashed line represent the m phase. Key: (■) D_c, (▲) $\langle D\rangle_a$ and (●) D_β and (c) Microstrain of sample A-X12 as a function of sintering temperature. Solid symbols and solid line correspond to the t phase, whereas the open symbols and dashed line represent the m phase. Key: (■) $\hat{e}$, (●) G and (▲) $\langle\varepsilon^2\rangle^{1/2}$.

higher than 1100 °C. One might argue that heterogeneous dopant distribution could be attributed to the presence of m phase formation. If this were the case, the distribution would tend to scatter, which is not observed in this study. Furthermore, a Vogel diagram for as-derived powders [9] demonstrates that the dopant concentration is rather homogeneous.

The kinetics of the t → m phase transformation could be considered to be burst-like and hence nucleation-controlled, if the t crystals are fully transformed into the m phase and also if the mean crystallite size of the t phase does not decrease due to the absence of partially transformed t crystals. However, partially transformed t crystals often exist which results in a decrease in the crystallite size of the t phase.

The correlation between the microstrain and sintering temperature has been shown by three different methods to be similar, as is shown in Fig. 2c. The microstrain of the t phase decreases, whereas that of the m phase is slightly altered as the sintering temperature is raised. It is known that the t → m phase transformation involves a 5% volume expansion of the t phase and that the lattice mismatch between the two phases leads to an increase in the microstrain in the m phase [28]. Thus, the m phase microstrain is larger than that of the t phase under the matrix constraint condition. The microstrain of the t phase can decrease due to (a) annealing effects and (b) strain relief resulting from the occurrence of the t → m transformation. The microstrain of m phase remains unchanged which is probably due to the constraints imposed by the neighbouring matrix.

3.3. Thermal degradation

Most concepts applied to the understanding of the mechanism of the kinetics of the t → m phase transformation in zirconia come from the study of metals and are therefore athermal [34]. Yoshimura [35] has suggested that the phase stability of zirconia should be considered with respect to both thermodynamic and kinetic aspects. However, the t → m phase transformation in doped zirconia exhibits isothermal characteristics. Nakaishi and Shigematsu [36] have reported that the kinetic characteristics depend on the valence state of the dopant. For example Y_2O_3 doped t zirconia exhibits an isothermal type transition, whilst CeO_2 doped t zirconia is a burst-like (athermal type) transition. When the crystallite size of t pure zirconia, is less than 100 nm, the t → m transition is isothermal, whilst at grain sizes larger than this the transition is athermal [37]. Subbarao *et al.* [38] have argued that this is the result of surface energy contributions.

Using XRD line profile analysis to investigate the microstructural relationship between the parent-t phase and the product-m phase phase is a new approach which can add to the information currently available from other techniques, such as differential thermal analysis (DTA) and transmission electron microscopy (TEM). If the microstructural relationship between the t and m phases can be understood, then it can help rationalize the evolution of isothermal and athermal type t → m phase transformations. The selection of 3 mol % CeO_2–ZrO_2 as the material for study is due to its monoclinic phase content of around 50 vol % after it has been annealed at 900 °C for 10 mins, as is shown in Table II. After this heat treatment the sample contains identical mean crystallite sizes of 10.9 nm for both the t and m phases. Table II lists the t and m crystallite sizes, microstrains and the volume percentage of the m phase in the 3 mol % CeO_2–ZrO_2 powders as a function of the holding time at 900 °C.

Powders produced by the urea-hydrolysis process and subsequent hydrothermal treatment contain 17 vol % monoclinic phase in the as-derived state. After heating at 900 °C for 120 min, the percentage of the monoclinic phase increases from 53 to 65 vol %. If the holding time is extended to 420 min, there is a slight increase in the monoclinic phase content to around 67 vol %. As the amount of the CeO_2 dopant is increased, the monoclinic phase content becomes less sensitive to the holding time at 900 °C, as is shown in Fig. 3a. According to the high temperature XRD results of Srinivasan *et al.* [39] during the cooling process after a heating at 800 °C, the metastable tetragonal phase of pure zirconia is progressively transformed into the monoclinic phase from 450 °C to room temperature. Thus, the monoclinic phase content observed in samples held at 900 °C can be either formed during the holding stage (isothermal type m phase) or on cooling (athermal type m phase). The existence of two kinds of monoclinic phase formation results in different microstructures of the m and t phases. It is believed that an isothermal type phase transformation can occur from pre-existing monoclinic plates which continue to grow. The holding

TABLE II The crystallite size and microstrain of 3 mol % CeO_2–ZrO_2 powder pellets held at 900 °C as a function of holding time.

Sample designation	Holding time (min)	Tetragonal content (vol %)	Tetragonal phase				Monoclinic phase			
			$2w_{Pv(L)}$ (nm)	Crystallite size $\langle D\rangle_a$ (nm)	$\langle D\rangle_v$[a] (nm)	Microstrain $\langle\varepsilon^2\rangle^{1/2}_{L=3.0\,nm}$ ($\times 10^2$)	$2w_{Pv(L)}$ (nm)	Crystallite size $\langle D\rangle_a$ (nm)	$\langle D\rangle_v$ (nm)	Microstrain $\langle\varepsilon^2\rangle^{1/2}_{L=3.0\,nm}$ ($\times 10^2$)
3mCe10	10	47	18.55	10.98	16.62	1.37	16.62	10.83	14.85	2.85
3mCe40	40	44	18.77	11.35	16.25	1.33	13.97	8.86	11.95	2.75
3mCe120	120	35	23.95	13.37	19.53	1.63	21.73	11.21	16.97	2.82
3mCe200	200	38	24.19	13.11	19.49	1.67	17.42	10.76	15.46	2.71
3mCe420	420	33	22.48	13.78	19.40	1.36	19.56	18.15	19.83	2.68

[a] The volume-weighted mean crystallite size and microstrain are calculated using the Warren–Averbach procedure.

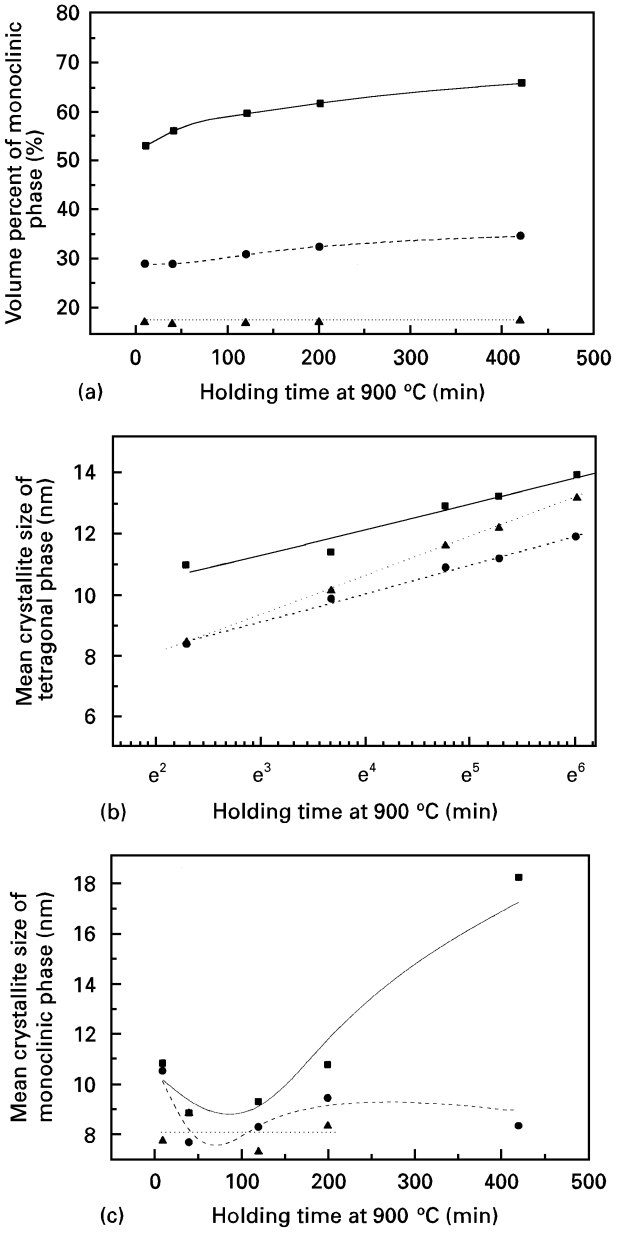

Figure 3 (a) The volume percent of m phase and mean crystallite size of, (b) t and, (c) m phases in CeO_2 doped zirconia as a function of holding time at 900 °C. Key (■) 3 mol % CeO_2, (●) 5.5 mol % CeO_2 and (▲) 7 mol % CeO_2.

stage creates two features of the microstructure of low Ce-doped zirconia: (i) the t phase crystals grow, and (ii) the isothermal t → m phase transformation occurs. The latter process can lead to an increase in both the mean size of the m crystals due to the growth of pre-existing m plates and also the nucleation sites for subsequent athermal t → m transformation during the cooling stage.

As indicated in Table II, the mean crystallite size for the t phase increases, whereas that of the m phase first decreases and then increases as the holding time increases from 10 to 420 min. Fig. 3(a–c) plots the mean crystallite size of the m phase in 3-, 5.5- and 7-mol % CeO_2 doped zirconia samples in terms of the holding time at 900 °C. As the holding time increases from 10 to 40 min the 3 mol % CeO_2–ZrO_2 and 5.5 mol % CeO_2–ZrO_2 samples exhibit a decrease in the mean crystallite size for the m phase, whilst it remains constant in the 7 mol % CeO_2–ZrO_2 sample. In the case of the as-sintered surface, the presence of the m phase and partition of the t phase results in a decrease of the mean crystallite size for the t phase. However, the t crystallite size for the low Ce-doped zirconia samples does not exhibit a similar decrease as that in the as-sintered surface for TZP. This can be attributed to the fact that the percentage of partially transformed t crystals is less and thus the size of the t crystals are not decreased. At the same time, the change in the mean size of the m phase crystallites is due to the occurrence of the isothermal type t → m transformation. On the basis of the above results, it is considered that if the temperature is held at 900 °C for a short time (say 10 min) then the isothermal t → m phase transformation may not occur. When the temperature is decreased from 900 °C to room temperature, the athermal t → m transition occurs on cooling. The m plates rapidly partition the t matrix since the t → m transition is nucleation-controlled. When the holding time at 900 °C is increased (longer than 10 min), the fraction of isothermal type m phase increases and the t crystals can grow. Subsequently, the athermal t → m transition occurs on cooling and the mean size of the m crystals depends on the size of the growing t crystals. Nevertheless, a small fraction of isothermal type t → m transformation that can occur after a short holding time (i.e., held for 40 min) can enhance the number of nucleation sites for the subsequent athermal t → m transformation, resulting in a decrease in the mean crystallite size of the m crystals. As the holding time is increased to 120 min or above, m crystals can grow from the pre-existing m plates, and this leads to an increase in the mean size of the m crystals. In addition, the growth of as-derived m crystals must be considered with respect to the holding time. There is no t → m phase transition in the 7 mol % CeO_2–ZrO_2 sample. Even if the sample is held at 900 °C for 200 min, no change in the mean size of the m phase crystallites is observed as is shown in Fig. 3c. Thus, the m crystals fail to grow even at the most extreme conditions that the sample is exposed to.

The distribution of crystallite sizes also reveals microstructural changes in the zirconia samples, as is evident in Fig. 4(a and b) and Table II. After the isothermal transformation, the width of the $P_v(L)$ curves for both the m and t phases increases. The maximum of the $P_v(L)$ curve for the t phase shifts towards larger L values, whereas that of the m phase initially moves towards lower L values and then towards larger L values, as the holding time is increased. These results are in agreement with the trends in the mean crystallite size.

The t → m phase transformation involves a 5% volume expansion, and thus the microstrain of the monoclinic crystal will depend on whether or not the monoclinic crystal is constrained by the matrix. When the lattice of the monoclinic crystal is unable to freely expand to relieve the transformation strain an increase in the microstrain in the monoclinic crystals to levels. greater than that in the parent-t crystal is observed. As can be seen in Table II, the microstrain levels in the m phase is larger than that of the t phase for all studied samples. It appears that the increase in holding time

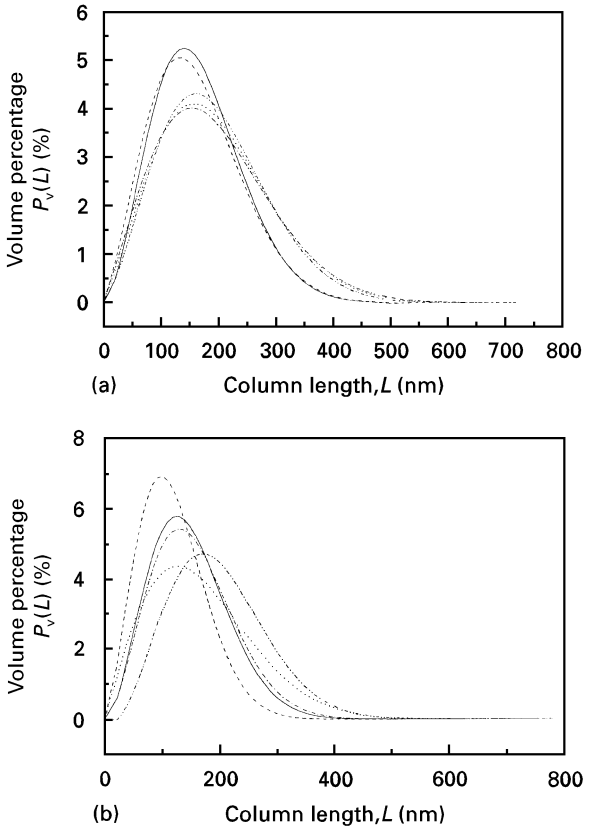

Figure 4 The distribution of crystallite size of (a) tetragonal phase and (b) monoclinic phase for 3 mol % CeO_2–ZrO_2 aged at 900 °C for (—) 10 min, (– –) 40 min, (----) 120 min, (–·–·) 200 min and (–··–··) 420 min.

does not affect the microstrain for both the t and m phases.

Finally, the microstructural relationship between the t and m phases in the t → m phase transformation is schematically summarized in Fig. 5(a and b) which illustrates the variation of the mean crystallite size for both the t and m phases with respect to treatment conditions. For a zirconia ceramic containing a few pre-existing m crystals, the t → m phase transformation can occur from either the untransformed or the partially transformed t crystals, as is indicated in Fig. 5(a and b), respectively. When the t → m phase transformation proceeds by isothermal or athermal processes, the variation of the mean crystallite size and $P_v(L)$, is as shown in Fig. 5(a and b). It should be noted that the partially transformed t crystals can significantly influence the mean crystallite size of the t phase.

4. Conclusions

(1) Powders with a composition of 5.5 mol % CeO_2–2 mol % $YO_{1.5}$–ZrO_2 derived by ammonia coprecipitation and subsequent calcination at 500 °C for 0.5 h contain 30 vol % of the monoclinic phase. The mean crystallite size of the m phase is smaller than that of the t phase due to constraints applied by the parent phase. The crystallite size of the m phase slightly increases whilst that of the t phase decreases as the t phase transformation proceeds due to the milling. This implies that some of the newly produced m plates created by stress, are thicker than the thermally-induced m phase. In addition, the distribution of the m phase crystallite size also becomes broadened by the ball milling.

(2) The monoclinic phase in the as-sintered surface of a 5.5 mol % CeO_2–2 mol % $YO_{1.5}$–ZrO_2 ceramic sintered at temperatures greater than 1300 °C exhibits preferred orientation that is similar to the ground surface of Y-doped zirconia. The presence of the m phase results in a decrease in the mean size of the t phase. Both the mean sizes of the t and m phases increase as the sintering temperature is raised to 1400 °C or above, which indicates that the t → m phase transformation occurs during heating at temperatures above 1100 °C at which point the partially transformed or partitioned t crystals are formed.

(3) Powders of lower Ce-doped zirconia exhibit an isothermal type t → m phase transformation during the holding period, while an athermal one occurs upon cooling. The occurrence of the t → m during the transformation holding period alters the subsequent athermal transition on cooling, resulting in a change in the mean size of the m crystals.

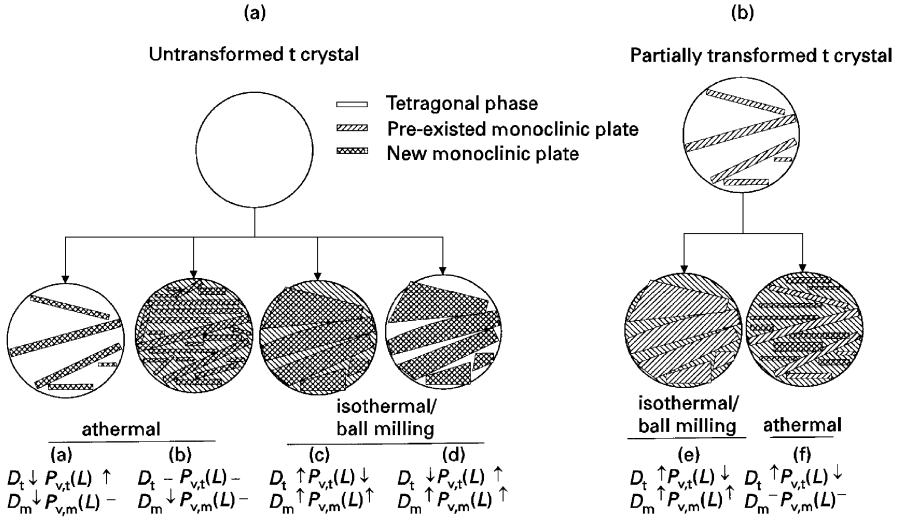

Figure 5 Schematic illustration of the evolution of the t and m crystallite sizes in the t-to-m phase transformation.

(4) The t → m phase transformation involves a 5% volume expansion, and thus the microstrain state of the m crystal depends on whether or not the crystal is constrained by the matrix. When the lattice of the m crystals cannot freely expand to relieve the transformation strain, then a microstrain larger than that of the parent crystal is produced. On the other hand, for isolated particles the microstrain of m crystallites is smaller than that for t crystallites.

(5) Samples of 5.5 mol % CeO_2–2 mol % $YO_{1.5}$–ZrO_2 contain 30 vol % m phase after a 12 h ball milling in alcohol. The microstrain of the m crystallites is larger than that of the t crystallites in the powder. This is due to the fact that the t phase can relieve the stress induced by the ball milling by the t → m phase transformation, whereas the m phase cannot relieve the stress and thus stress is accumulated, resulting in a high microstrain.

Acknowledgement

The authors are grateful for financial support from the National Science Council, Taiwan under contracts no. NSC82-0425-E-007-188 and NSC83-0405-E-007-017.

References

1. R. H. J. HANNINK and M. V. SWAIN, *Ann. Rev. Mater. Sci.* **24** (1994) 359.
2. M. RÜHLE and A. G. EVANS, *Prog. Mater. Sci.* **33** (1987) 85.
3. S. LAWSON, *J. Eur. Ceram. Soc.* **15** (1995) 485.
4. A. H. HEUER, N. CLAUSSEN, W. M. KRIVEN and M. RÜHLE, *J. Amer. Ceram. Soc.* **65** (1982) 642.
5. F. F. LANGE, *J. Mater. Sci.* **17** (1982) 225.
6. R. C. GARVIE and M. V. SWAIN, *ibid* **20** (1985) 1193.
7. *Idem*, *ibid* **20** (1985) 3479.
8. J. D. LIN and J. G. DUH, *J. Amer. Ceram. Soc.* **80** (1997) 92.
9. *Idem*, *J. Mater. Sci.* (accepted).
10. R. H. J. HANNINK, B. C. MIDDLE and M. V. SWAIN, in Proceedings Austceram '86, Australian Ceramic Society, Melbourne, Australia, 1986, p. 145.
11. D. J. GREEN, R. H. J. HANNINK and M. V. SWAIN, in "Transformation toughening of ceramics", (CRC Press, Boca Raton, Florida, 1989) p. 144.
12. M. RÜHLE, N. CLAUSSEN and A. H. HEUER, in "Advances in ceramics, Vol. 12. Science and technology of zirconia II", edited by N. Claussen, M. Rühle and A. H. Heuer (The American Ceramic Society, Columbus, OH, 1984) p. 352.
13. R. H. J. HANNINK and M. V. SWAIN, *J. Amer. Ceram. Soc.* **72** (1989) 90.
14. H. ZHU, *ibid* **77** (1994) 2458.
15. P. E. REYES-MOREL and I.-W. CHEN, *ibid* **71** (1988) 343.
16. B. E. WARREN, *Prog. Metal Phys.* **8** (1959) 147.
17. R. DELHEZ, TH. H. DEKEIJSER and E. J. MITTEMEIJER, *Fresenius Z. Anal. Chem.* **312** (1982) 1.
18. J. G. DUH, H. T. DAI and B. S. CHIOU, *J. Amer. Ceram. Soc.* **71** (1988) 813.
19. J. G. DUH, H. T. DAI and W. Y. HSU, *J. Mater. Sci.* **23** (1988) 2786.
20. J. G. DUH and M. Y. LEE, *ibid.* **24** (1989) 4467.
21. J. G. DUH and Y. S. WU, *J. Mater. Sci. Lett.* **10** (1991) 1003.
22. J. G. DUH and J. U. WAN, *J. Mater. Sci.* **27** (1992) 6197.
23. *Idem*, *J. Mater. Sci. Lett.* **12** (1993) 575.
24. H. TORAYA, M. YOSHIMUREA and S. SOMIYA, *J. Amer. Ceram. Soc.* **67** (1984) C-119.
25. J. E. BAILEY, D. LEWIS, Z. M. LIBRANT and L. J. PORTOR, *Trans. J. Brit. Ceram. Soc.* **71** (1972) 25.
26. Y. MURASE and E. KATO, *J. Amer. Ceram. Soc.* **62** (1979) 527.
27. J. S. REED, in "Introduction to the principles of ceramic processing", (John Wiley, New York, 1989) Ch. 16.
28. A. van RIESEEN and B. H. O'CONNOR, *J. Amer. Ceram. Soc.* **76** (1993) 2133.
29. A. H. HEUER and M. RÜHLE, *Acta. Metall.* **33** (1985) 2101.
30. M. RÜHLE and A. H. HEUER, in "Advances in ceramics, Vol. 12. Science and technology of zirconia II", edited by N. Claussen, M. Rühle and A. H. Heuer, (The American Ceramic Society, Columbus, OH, 1983) p. 14.
31. R. SRINIVASAN, L. RICE and B. H. DAVIS, *J. Amer. Ceram. Soc.* **73** (1990) 3528.
32. B. MOROSIN, R. A. GRAHAM, Y. ZHANG, J. M. STEWART and C. R. HUBBARD, *Aust. J. Phys.* **41** (1988) 251.
33. M. V. SWAIN and R. H. J. HANNINK, *J. Amer. Ceram. Soc.* **72** (1989) 1358.
34. Z. NISHIYAMA, in "Martensitic transformations", edited by M. E. Fine, M. Meshii and C. M. Wayman (Academic Press, New York, 1978) p. 275.
35. M. YOSHIMURA, *Amer. Ceram. Bull.* **67** (1988) 1950.
36. N. NAKANISHI and T. SHIGEMATSU, *Mat. Trans. JIM* **33** (1992) 318.
37. H. S. MAITI, K. V. G. K. GOKNALE and E. C. SUBBARAO, *J. Amer. Ceram. Soc.* **55** (1972) 317.
38. E. C. SUBBARAO, H. S. MAITI and K. K. SRIVASATAVA, *Phys. Stat. Sol.* (*a*) **21** (1974) 9.
39. R. SRINIVASAN, C. R. HUBBARD, O. B. CAVIN and B. H. DAVIS, *Chem. Mater.* **5** (1993) 27.

Received 25 March 1996
and accepted 21 March 1997